Available online at www.sciencedirect.com
ScienceDirect
Physica E 40 (2008) 1404–1406
PHYSICA E
www.elsevier.com/locate/physe

Corner multifractality for reflex angles and conformal invariance at 2D Anderson metal–insulator transition with spin–orbit scattering

H. Obuse[a,*], A.R. Subramaniam[b], A. Furusaki[a], I.A. Gruzberg[b], A.W.W. Ludwig[c]

[a]Condensed Matter Theory Laboratory, RIKEN, Wako, Saitama 351-0198, Japan
[b]James Franck Institute, University of Chicago, 5640 South Ellis Avenue, Chicago, IL 60637, USA
[c]Physics Department, University of California, Santa Barbara, CA 93106, USA

Available online 19 September 2007

Abstract

We investigate boundary multifractality of critical wave functions at the Anderson metal–insulator transition in two-dimensional disordered non-interacting electron systems with spin–orbit scattering. We show numerically that multifractal exponents at a corner with an opening angle $\theta = 3\pi/2$ are directly related to those near a straight boundary in the way dictated by conformal symmetry. This result extends our previous numerical results on corner multifractality obtained for $\theta < \pi$ to $\theta > \pi$, and gives further supporting evidence for conformal invariance at criticality. We also propose a refinement of the validity of the symmetry relation of A.D. Mirlin et al. [Phys. Rev. Lett. 97 (2006) 046803] for corners.

PACS: 73.20.Fz; 05.45.Df; 72.15.Rn

Keywords: Conformal invariance; Anderson transition; Multifractality; Spin–orbit interaction

Anderson metal–insulator transitions are continuous phase transitions driven by disorder. Examples of localization–delocalization (Anderson) transitions occurring in two dimensions (2D) include non-interacting electronic systems with spin–orbit scattering ('symplectic symmetry class'), with sublattice symmetry, or in strong magnetic fields (quantum Hall effect).

Recently, we have reported numerical evidence for the presence of conformal invariance at the 2D Anderson transition in the symplectic symmetry class [1]. To that end, we have considered multifractal properties of critical wave functions near boundaries of disordered samples of finite size, and verified numerically that the multifractal exponents of critical wave functions at corners with opening angle θ (corner multifractality) are related, through simple relations derived from conformal invariance, to the exponents computed near straight edges (surface multifractality). In Ref. [1] we have discussed corner multifractality at wedges with angles $\theta < \pi$ only, both acute ($\theta = \pi/4$) and obtuse ($\theta = 3\pi/4$). In this paper we extend this analysis to a corner with $\theta = 3\pi/2$ to show that the same equation relating surface and corner multifractality holds for the corner with a reflex angle ($\theta > \pi$).

Following Refs. [1,2], we define bulk, surface, and corner multifractality from the scaling of moments of wave functions $\psi(\boldsymbol{r})$ in bulk (b), surface (s), and corner (θ) regions,

$$L^{d_{\mathrm{x}}}\overline{|\psi(\boldsymbol{r})|^{2q}} \sim L^{-\tau_q^{\mathrm{x}}} \quad (\mathrm{x} = \theta, \mathrm{s}, \mathrm{b}), \tag{1}$$

where d_{x} is the spatial dimension of each region ($d_{\mathrm{b}} = 2$, $d_{\mathrm{s}} = 1$, and $d_\theta = 0$). The overbar represents the ensemble (disorder) average and the simultaneous spatial average over a region x surrounding the point $\boldsymbol{r}$. The exponents τ_q^{b}, τ_q^{s}, and τ_q^{θ} are the bulk, surface, and corner multifractal exponents, respectively. From the multifractal exponents we extract non-vanishing anomalous dimensions Δ_q^{x},

$$\Delta_q^{\mathrm{x}} = \tau_q^{\mathrm{x}} - 2q + d_{\mathrm{x}}. \tag{2}$$

*Corresponding author. Tel.: +81 48 462 1111; fax: +81 48 467 1339.
E-mail address: obuse@riken.jp (H. Obuse).

1386-9477/$ - see front matter © 2007 Elsevier B.V. All rights reserved.
doi:10.1016/j.physe.2007.09.024

The multifractal singularity spectra $f^{\mathrm{x}}(\alpha)$ are obtained from τ_q^{x} by Legendre transformation

$$f^{\mathrm{x}}(\alpha^{\mathrm{x}}) = \alpha^{\mathrm{x}} q - \tau_q^{\mathrm{x}}, \quad \alpha^{\mathrm{x}} = \frac{\mathrm{d}\tau_q^{\mathrm{x}}}{\mathrm{d}q}. \tag{3}$$

As explained in Ref. [1], under the assumption that the qth moment $|\psi(\boldsymbol{r})|^{2q}$ is represented by a primary operator in an underlying conformal field theory [3], one can derive, using the conformal mapping $w = z^{\theta/\pi}$, the relation between the surface and corner multifractal spectra $f^{\mathrm{x}}(\alpha_q^{\mathrm{x}})$,

$$\alpha_q^{\theta} - 2 = \frac{\pi}{\theta}(\alpha_q^{\mathrm{s}} - 2), \quad f^{\theta}(\alpha_q^{\theta}) = \frac{\pi}{\theta}[f^{\mathrm{s}}(\alpha_q^{\mathrm{s}}) - 1]. \tag{4}$$

The validity of these relations provides direct evidence for conformal invariance at a 2D Anderson transition and for the primary nature of the operator.

In Ref. [1] we have shown that the probability distribution of $\ln|\psi(\boldsymbol{r})|^2$ becomes broader, as the opening angle θ is reduced. This implies that the distribution is narrower at a corner with larger θ. We may thus expect that multifractal exponents can be more accurately calculated for corners with reflex angles than for corners with angles $\theta < \pi$. We can then estimate the surface $f^{\mathrm{s}}(\alpha_q^{\mathrm{s}})$ by taking the numerical data for α_q^{θ} and $f^{\theta}(\alpha_q^{\theta})$ obtained for $\theta > \pi$ as input into Eq. (4). Moreover, we can relate multifractal spectra of corners with different angles θ and θ' ($\theta < \theta'$), yielding

$$\alpha_q^{\theta} - 2 = \frac{\theta'}{\theta}(\alpha_q^{\theta'} - 2), \quad f^{\theta}(\alpha_q^{\theta}) = \frac{\theta'}{\theta} f^{\theta'}(\alpha_q^{\theta'}). \tag{5}$$

As we pointed out in Ref. [1], Eqs. (4) and (5) are valid only if all occurring $\alpha_q^{\mathrm{x}} \geqslant 0$, because α_q^{x} is non-negative for normalized wave functions. Thus, when the prefactor θ'/θ is larger than one (and hence $0 \leqslant \alpha_q^{\theta} < \alpha_q^{\theta'}$), the first of Eq. (5) cannot be used for $q > q_{\theta}$, where q_{θ} is a solution to $\alpha_q^{\theta} = 0$ in Eq. (5). (We do not know if q_{θ} is finite for $\theta \geqslant \pi$). Taking this physical constraint into account, we find the following relation between anomalous dimensions for corners ($\theta < \theta'$),

$$\Delta_q^{\theta} = \begin{cases} \dfrac{\theta'}{\theta}\Delta_q^{\theta'}, & q \leqslant q_{\theta}, \\ \dfrac{\theta'}{\theta}\Delta_{q_{\theta}}^{\theta'} - 2(q - q_{\theta}), & q > q_{\theta}. \end{cases} \tag{6}$$

If we set $\theta = \pi$ in Eq. (6), we obtain a relation between anomalous dimensions at a surface ($\theta = \pi$) and a corner with a reflex angle ($\theta' > \pi$). In Ref. [1] we also discussed the symmetry relation of Ref. [4], $\Delta_q^{\mathrm{x}} = \Delta_{1-q}^{\mathrm{x}}$, and its application to corners $\mathrm{x} = \theta$. Here we propose, as a refinement of that discussion, that this symmetry relation (i) is valid for corners of any angle θ including $\theta = \pi$ (straight boundaries), but only in the range of q satisfying $1 - q_{\theta} \leqslant q \leqslant q_{\theta}$, corresponding precisely [1,4] to the range $0 \leqslant \alpha_q^{\theta} \leqslant 4$, and (ii) makes no statements about Δ_q^{θ} for values of q outside of this range. [The dependence on q of Δ_q^{θ} is linear for $q > q_{\theta}$ (corresponding to the termination of the multifractal spectrum [5]), whilst it may, in general, continue to be non-linear for $q < 1 - q_{\theta}$, even [1,4] when $\alpha_q^{\theta} > 4$.]

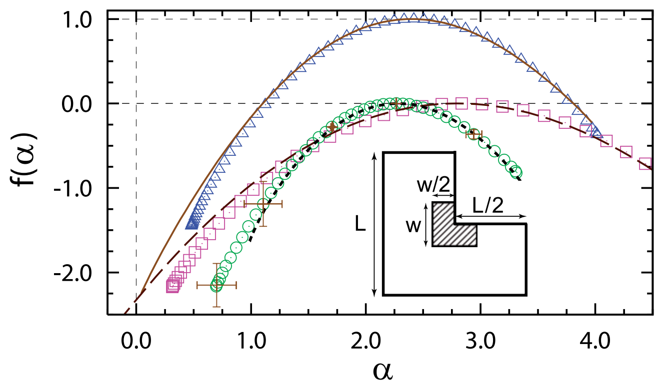

Fig. 1. (Color online) Multifractal spectra $f(\alpha)$ for corners with $\theta = 3\pi/2$ (circles) and $\theta = \pi/2$ (squares), and surface (triangles) regions. Error bars are plotted at integer values of q for the corner with $\theta = 3\pi/2$. The solid and short-dashed curves represent the theoretical prediction from Eq. (4), where $f^{3\pi/2}(\alpha_q^{3\pi/2})$ and $f^{\mathrm{s}}(\alpha_q^{\mathrm{s}})$ are used as input, respectively. The dashed curve is calculated from Eq. (5) with $f^{3\pi/2}(\alpha_q^{3\pi/2})$ used as input. Inset: L-form geometry with $3L^2/4$ sites. The shaded part is the corner region with $\theta = 3\pi/2$ of the size $3w^2/4$.

In this work, we numerically verify these relations by computing corner multifractal spectra at $\theta = 3\pi/2$ for the L-shape samples shown in the inset of Fig. 1. We take a tight-binding model with both random on-site potential and random SU(2) hopping [6], and numerically obtain, with the forced oscillator method [7], a wave function ψ having energy eigenvalue closest to a critical point $E_{\mathrm{c}} = 1.0$ (in units of the mean hopping) for each random realization characterized by the on-site disorder strength $W_{\mathrm{c}} = 5.952$. The system size L is varied through $L = 24, 30, \ldots, 120$ and the number of disordered samples is 6×10^4 for each L. We set $w = 2$ of the corner region shown in Fig. 1. Multifractal spectra are computed in the same way as in Ref. [1].

In Fig. 1, we show multifractal spectra $f(\alpha)$ of corners with $\theta = 3\pi/2$, together with those of corners with $\theta = \pi/2$, and of the surface region [1]. The peak position α_0^{x} of $f^{3\pi/2}(\alpha_q^{3\pi/2})$ is $\alpha_0^{3\pi/2} = 2.265 \pm 0.003$, which is smaller than $\alpha_0^{\pi/2} = 2.837 \pm 0.003$. Also, the width of $f^{3\pi/2}(\alpha)$ is smaller than that of $f^{\mathrm{s}}(\alpha_q^{\mathrm{s}})$. This is consistent with Eq. (4) at $\theta = 3\pi/2$. Fig. 1 clearly shows that $f^{3\pi/2}(\alpha)$ computed directly for the corner with $\theta = 3\pi/2$ agrees well with the short-dashed curve obtained from Eq. (4) while using $f^{\mathrm{s}}(\alpha)$ as input, which verifies Eq. (4) derived from conformal invariance. We have also calculated the surface $f^{\mathrm{s}}(\alpha_q^{\mathrm{s}})$ and corner $f^{\pi/2}(\alpha_q^{\pi/2})$ from Eqs. (4) and (5), respectively, using $f^{3\pi/2}(\alpha_q^{3\pi/2})$ as input into these equations. This allows us to estimate $f^{\mathrm{s}}(\alpha_q^{\mathrm{s}})$ near $\alpha^{\mathrm{s}} \approx 0$, providing an estimate for $q_{\mathrm{s}} = \mathrm{d}f^{\mathrm{s}}(\alpha^{\mathrm{s}} = 0)/\mathrm{d}\alpha^{\mathrm{s}}$. The theoretical predictions (solid and dashed curves) are in good agreement with the numerical data (triangles and squares) for $f^{\mathrm{s}}(\alpha_q^{\mathrm{s}})$ and $f^{\pi/2}(\alpha_q^{\pi/2})$, respectively.

Fig. 2 shows the anomalous dimensions Δ_q^{x} for corners with $\theta = 3\pi/2$ and $\theta = \pi/2$, and the surface region, which are numerically calculated from the scaling

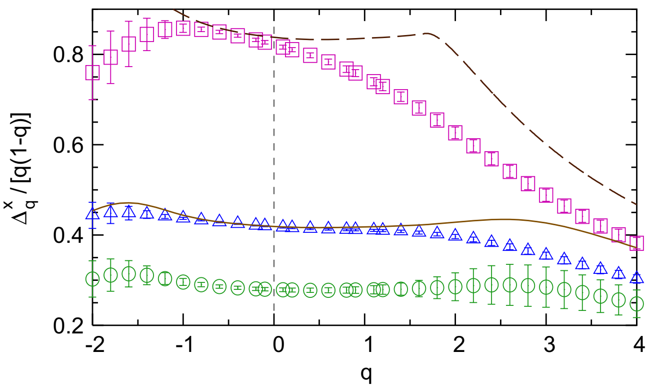

Fig. 2. (Color online) The exponents $\Delta_q^{\mathrm{x}}/[q(1-q)]$ for corner with $\theta = 3\pi/2$ (circles) and $\theta = \pi/2$ (squares), and surface (triangles) regions. Solid and dashed curves represent the conformal relation (6).

$\overline{|\psi(\boldsymbol{r})|^{2q}}/(\overline{|\psi(\boldsymbol{r})|^2})^q \sim L^{-\Delta_q^{\mathrm{x}}}$. The solid and dashed curves represent the theoretical prediction, Eq. (6), from the conformal mapping using $\Delta_q^{3\pi/2}$ as inputs. The data points for Δ_q^{s} (triangles) agree with the solid curve for $|q| \lesssim 1.5$, while those for $\Delta_q^{\pi/2}$ (squares) are close to the dashed curve only near $q \approx 0$. The data points for $\Delta_q^{3\pi/2}$ satisfy, within error bars, the symmetry relation [4] $\Delta_q^{3\pi/2} = \Delta_{1-q}^{3\pi/2}$ in the vicinity of $q = \frac{1}{2}$, indicating good numerical accuracy. This opens the possibility that one can use corner multifractality for $\theta > \pi$ to obtain, with the help of Eqs. (4) and (6), more accurate estimates for multifractal properties at a straight surface and corners with $\theta < \pi$.

We briefly comment on multifractality of a whole sample with boundaries. We have found in Refs. [1,2] that corner multifractality may dominate multifractality of a whole system, even in the thermodynamic limit, for large values of $|q|$ if $\tau_q^\theta < \tau_q^{\mathrm{b}}, \tau_q^{\mathrm{s}}$. Here we point out that this cannot happen with corners of reflex angles ($\theta > \pi$). The proof goes as follows. We first note that, from Eqs. (2) and (6), the difference of corner and surface multifractal exponents is given by $\tau_q^\theta - \tau_q^{\mathrm{s}} = 1 + \Delta_q^{\mathrm{s}}(\pi/\theta - 1)$ as long as $\alpha_q^{\mathrm{s}} > 0$ (note that $\alpha_q^\theta > \alpha_q^{\mathrm{s}}$ for $\theta > \pi$). Thus, when $\pi < \theta < 2\pi$, the inequality $\tau_q^\theta > \tau_q^{\mathrm{s}}$ holds if $\Delta_q^{\mathrm{s}} \leqslant 2$. Secondly, since τ_q^{x} is a convex function of q with the constraints $\tau_0^{\mathrm{x}} = -d_{\mathrm{x}}$ and $\tau_1^{\mathrm{x}} = 2 - d_{\mathrm{x}}$ (recalling [1] $\mu = 0$, and thus $\Delta_1^{\mathrm{x}} = 0$), we find $\Delta_q^{\mathrm{x}} \leqslant 0$ for $|q - 1/2| \geqslant 1/2$ and $0 < \Delta_q^{\mathrm{x}} < 2$ for $0 < q < 1$. We thus conclude that $\tau_q^\theta > \tau_q^{\mathrm{s}}$ when $\alpha_q^{\mathrm{s}} > 0$. Finally, when $\tau_q^\theta - \tau_q^{\mathrm{s}}$ is positive for $\alpha_q^{\mathrm{s}} > 0$ the difference remains positive even if $q_{\mathrm{s}} < \infty$ and in the regime $q \geqslant q_{\mathrm{s}}$ where $\alpha_{q_{\mathrm{s}}}^{\mathrm{s}} = 0$, because τ_q^{s} is then constant for $q \geqslant q_{\mathrm{s}}$ (and $\mathrm{d}\tau_q^\theta/\mathrm{d}q = \alpha_q^\theta \geqslant \alpha_q^{\mathrm{s}}$). Hence, contributions from corner multifractality at $\theta > \pi$ cannot be larger than contributions from surface multifractality. The numerical results shown in Fig. 1 are consistent with the above general argument.

In summary, we have investigated corner multifractality for the reflex angle $\theta = 3\pi/2$ and confirmed the validity of the conformal symmetry relations. This result provides stronger evidence for the presence of conformal symmetry at the 2D Anderson metal–insulator transition with spin-orbit scattering.

This work was supported by NAREGI grant from MEXT of Japan, the NSF under Grant no. PHY99-07949, the NSF MRSEC under no. DMR-0213745, the NSF Career Grant no. DMR-0448820, and Research Corporation. Numerical calculations were performed on the RIKEN Super Combined Cluster System.

References

[1] H. Obuse, A.R. Subramaniam, A. Furusaki, I.A. Gruzberg, A.W.W. Ludwig, Phys. Rev. Lett. 98 (2007) 156802.
[2] A.R. Subramaniam, I.A. Gruzberg, A.W.W. Ludwig, F. Evers, A. Mildenberger, A.D. Mirlin, Phys. Rev. Lett. 96 (2006) 126802.
[3] A.A. Belavin, A.M. Polyakov, A.B. Zamolodchikov, Nucl. Phys. B 241 (1984) 333.
[4] A.D. Mirlin, Y.V. Fyodorov, A. Mildenberger, F. Evers, Phys. Rev. Lett. 97 (2006) 046803.
[5] F. Evers, A.D. Mirlin, arXiv:0707.4378 (unpublished).
[6] Y. Asada, K. Slevin, T. Ohtsuki, Phys. Rev. Lett. 89 (2002) 256601; Y. Asada, K. Slevin, T. Ohtsuki, Phys. Rev. B 70 (2004) 035115.
[7] T. Nakayama, K. Yakubo, Phys. Rep. 349 (2001) 239.